Kinetic and Equilibrium Investigation of the Proton Uptake Process in the Complex Formation between Counter-Charged Ionic Polypeptides

Takayuki SANO,* Thoru NAKATSUKA, and Katsuaki INOUE
Department of Materials Science, Faculty of Science, Hiroshima University, Higashi-Hiroshima, 724
(Received August 9, 1993)

To clarify the mechanism of polymer complex formation between counter-charged polymers, kinetic and equilibrium experiments concerning the complexation of poly(L-α-glutamic acid) (PGA) with poly (L-α-lysine) (PLL) were performed at around pH 5.5 by the stopped-flow method. The reaction kinetics observed with electric conductivity detection and direct proton detection using the hydrogen ion-sensitive field-effect transistor suggests that the complex formation between these polymers proceeds through two processes of a fast proton release within 10 ms and a slow proton uptake within a few seconds. Further experiments using the various chain lengths of PGA and a variety of combinations of polymers and their counter-charged small ion, (e.g., PGA and amines or metal ions, PLL and carboxylic acids) have revealed that slow proton uptake in their complex formation is specific for a system which includes both a polymer and its counter-charged ions of divalent or more, and that this proton uptake is due to rearrangement of the polymer after fast electrostatic binding as a cooperative process.

Polymer–polymer complex formations, which bring about new properties that are different from those of its components, have been widely investigated[1—3] from the viewpoints of not only physical chemistry, but also polymer engineering. The polymer–polymer interaction is important for any profound understanding of the complicated mechanisms in biological systems, such as protein–protein interactions, DNA–protein interaction, and enzyme reactions.[4—6] Among the non-covalent binding between ionic polymers, the electrostatic long-range interaction must be predominant in the primary step of their complex formation; then, such short-range interactions as hydrophobic, hydrogen bonding, play the role of stabilizing the complex. Although kinetic studies in the polymer–polymer system facilitate an elucidation of the mechanism of polymer complexation, quite restricted kinetic studies have been reported[7—9] in contrast to a large amount of static or equilibrium investigations available. We thus carried out kinetic experiments concerning complexation formation between two polypeptides of poly (L-α-glutamic acid) (PGA) and poly (L-α-lysine) (PLL) as typical anionic and cationic polymers, respectively. Concerning PGA–PLL complexation around neutral pH, proton release from the side chain of PGA has been confirmed statically;[10—13] we expected to pursue the complex formation reaction by detecting the proton release. In practice, although we have observed the kinetic process accompanying the concentration change of a proton,[14] the direction of the change in the proton concentration was in contrast to our expectation regarding proton release. A proton uptake process was virtually observed in additon to the fast proton release beyond the resolution time of the present apparatus. This behavior of the proton is of interest, since proton release and uptake have been observed in many biochemical reactions such as enzyme-substrate interactions,[15,16] and proton pumps.[17,18] In the present paper, we elucidate the fundamental mechanism of proton uptake on polymer complexation through both kinetic and equilibrium experiments for various combinations, such as polymer–polymer, polymer–small ion, and small ion–small ion.

Experimental

Materials: PGA sodium salts with degrees of polymerization (DP) of 10, 60, and 250 were kindly supplied from Ajinomoto Co., Inc. and the hydrobromide salts of PLL (DP=460) were purchased from Sigma Chem. Co. The polymers were dialyzed against deionized water and lyophilized. The other chemicals used were of reagent grade and were used without further purification.

Apparatus: Kinetic experiments were undertaken mainly using a conductivity detection stopped-flow apparatus having a dead time of 15 ms.[19] A stopped-flow apparatus incorporated with a hydrogen-ion sensitive-field effect transistor for the direct observation of the proton behavior on polymer complex formation was also used. The dead time of this apparatus was 3 ms and a solution of 0.2 ml was necessary for each run. Details concerning the apparatus have been reported elsewhere.[20] We also used an optical detection stopped-flow apparatus to observe the hydrogen ion behavior with a pH indicator. A dicrhograph (Jobin-Yvon Mark III-J) was used for circular dichroism (CD) measurements of polymers. A capillary-type isotachophoresis apparatus (Shimadzu IP-2A) was used to determine the concentration of free small ions in the binding equilibrium.

Measurements: The pH-stat titration and equilibrium dialysis experments were undertaken on a PLL–glutaric acid system in order to estimate the binding constant and stoichiometric parameter at pH 5.5. The pH of solution was adjusted with a NaOH or HBr solution without the use of a pH buffer. The total pH change for the complexation was estimated to be the difference between the pHs before and after the reaction. Two sample solutions of the same volume and pH (5.5), where PGA is in the equilibrium of protolysis reaction of carboxylic acid while PLL is mostly protonated, were mixed with each other. We extended the experiments to systems which included a polymer and a small ion (e.g., PGA–amines or metal ions) and PLL–carboxylic acids un-

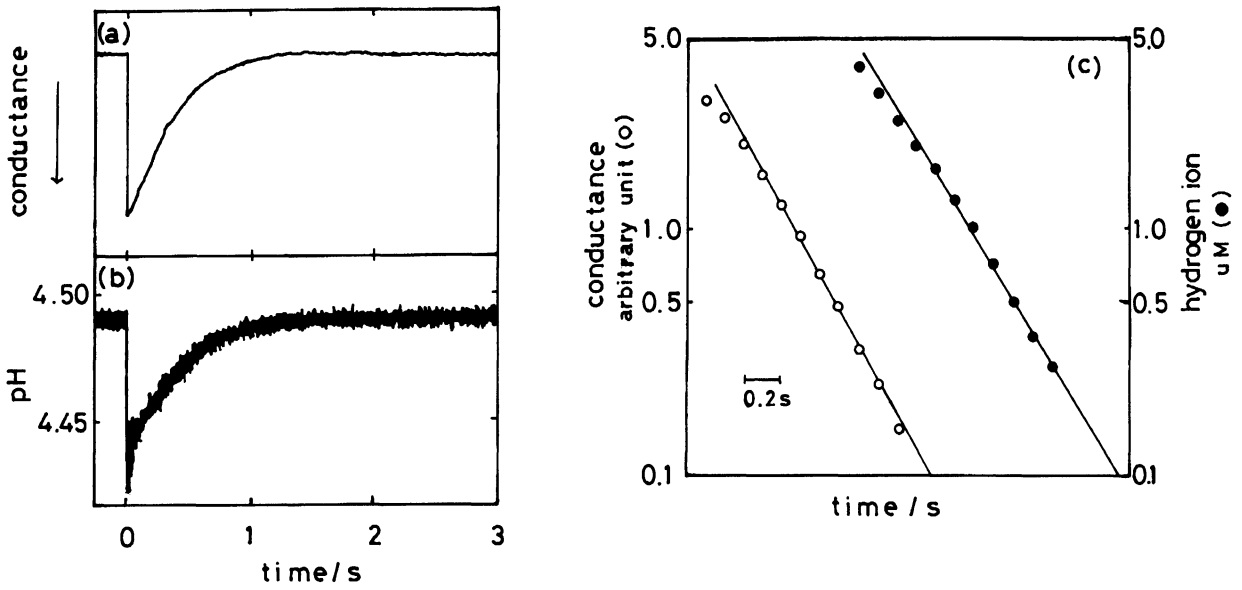

Fig. 1. Reaction curve and its semilogarithmic plot for the complexation between PGA and PLL at 1.0×10^{-4} M in residue unit. (a) Conductance detection; the downward arrow indicates increase in conductance, (b) pH detection, and (c) Semilogarithmic plots of the reaction curve versus time; the slope give the time constant τ. The values were estimated to be 3.0×10^{-1} s and 3.3×10^{-1} s for the conductance detection and pH detection, respectively.

der the same experimental conditions as for the polymer–polymer system. A PGA of DP=250 was mainly used in the present experiments; those of DP=60 and 10 were used only as a reference for a kinetic study of complexation with PLL. All of the experiments were performed at 25 °C and under the conditons of pH and concentration of each reaction species, which avoid any precipitation of the complex, at least during the reaction examined.

Results

A) Polymer–Polymer System. The reaction curves, observed by conductance and pH detections for the PGA (DP=250)–PLL system, are represented in Fig. 1(a) and (b). Only one kinetic curve with almost same time constant was observed for both measurements (Fig. 1(c)). Hence, the observed reaction as a conductance decrease corresponds to a proton-uptake process. On the other hand, since no reaction other than the first process was observed, the proton-release process must be much faster than the resolution time of the present apparatus (3 ms). Accordingly, it is obvious that complexation occurs through at least two steps of proton release and uptake. The time constant (τ) of the reaction was estimated by a semi-logarithmic plot of the reaction amplitude against time. The concentration dependencies of the time constant are given in Fig. 2. To examine the chain-length effect of the polymer on complexation, kinetic experiments were continued by using various degrees of polymerization of PGA (DPs=250, 60, and 10). We obtained similar results concerning both the time constant and the reaction amplitude, even low DP=10 of PGA (data not shown). This implies that the proton release and uptake are not necessarily specific for polymer–polymer complexation. Hence, we examined the behavior of the proton in systems which include small molecules and/or the polymers. The results of the kinetic experiments and proton-release measurements were summarized in Table 1.

B) Polymer-Small Ion System. Meanwhile, for combinations of 1) PLL–dicarboxylic acids, and 2) PGA–diamines and divalent metal ions, such as Ca^{2+} and Cu^{2+}, the proton uptake-process was observed. Static experiments, further, showed that the amount of proton release in the polymer–monovalent ions complex formation is smaller than that in the polymer–divalent ions complex formation. These experiental findings suggest that the interaction of the polymer with monovalent ions was obviously weaker than that with divalent ions. This result is coincident with the generally recognized fact that monovalent ions have a smaller tendency to form a complex electrostatically with other ions than divalent ions. Additionally, the proton-uptake process was not detected in the mixing of two small ions of dicarboxylic acids (DCA) and diamines (DAM). Thus, a combination of polymer and its counter-charged ions of divalent or more seems to be necessary for the proton-uptake and proton-release. The concentration dependence of the relaxation time is shown in Figs. 3 and 4 for the PLL–DCA and PGA–DAM systems, respectively.

C) Analysis of Kinetic Data. For an elucidation of the proton-uptake mechanism in the polymer–polymer system, a polymer–small ion system must give important information, because of the similar behavior of the proton in both systems. In this sense, we first examined the mechanism for polymer–small ion complex-

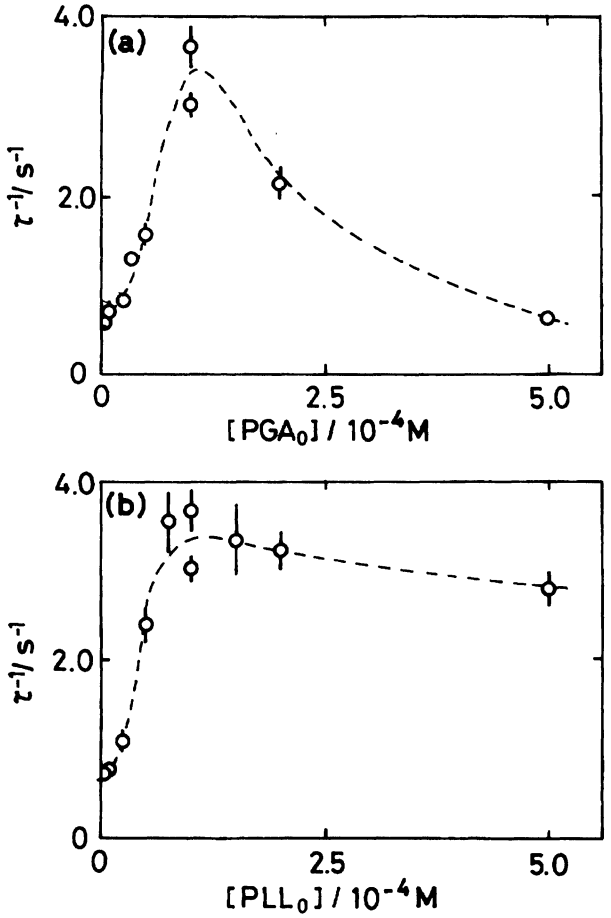

Fig. 2. The concentration dependence of the time constant τ for the PGA–PLL system. (a) $[PGA_0]$ dependence at $[PLL_0]=1.0\times10^{-4}$ M. (b) $[PLL_0]$ dependence at $[PGA_0]=1.0\times10^{-4}$ M. DP's of PLL and PGA are 460 and 250, respectively.

ation, and will extend the mechanism to the polymer–polymer system.

i) PLL–DCA System: The results of the pH-stat experiments for the PLL–glutaric acid system along with that of the equilibrium dialysis experiments are given in Fig. 5. For the determination of the binding parameters for complexation between PLL and glutaric acid (GL), the following two steps of proton dissociation of GL should be considered:

$$AH_2 \underset{H^+}{\overset{K_{a1}}{\rightleftarrows}} AH^- \underset{H^+}{\overset{K_{a2}}{\rightleftarrows}} A^{2-} \tag{1}$$

with

$$K_{a1}=\frac{[AH_2]}{[AH][H]}, \quad \text{and} \quad K_{a2}=\frac{[AH]}{[A][H]},$$

where AH_2, AH, and A denote the undissociate, monoanionic and dianionic species of GL, respectively. H denotes the hydrogen ion. Hereinafter, the signs of each ionic charge are omitted. On the other hand, since PLL is almost protonated at pH 5.5, it electrostatically interacts with GL in the form of either AH or A in Eq. 1.

First of all, for complexation between PLL and GL, the overall binding constant (K_{ov}) and stoichiometric coefficient (n) were estimated to satisfy the pH-stat data. The details concerning the determination of K_{ov} and n are given in Appendix 1. As a result, the values of $K_{ov}=1.7\times10^5$ M^{-1} and $n=0.45$ based on the following reaction scheme gave the most satisfactory curve fitting for the pH-stat data in Fig. 5(a) (1 M=1 mol dm^{-3}):

$$P + A \overset{K_{ov}}{\rightleftarrows} C \tag{2}$$

with

$$K_{ov}=\frac{[C]}{(n[PLL_0]-[C])[A]}, \tag{3}$$

where P denotes the binding site on the PLL, A the dianionic form of GL, and C the complex, respectively; n is the number of binding sites per one residue of the PLL for the A, $[PLL_0]$ the total concentration of PLL in the residue unit, [A] and [C] the concentration of the free dianionic form of GL and of the complex, respectively. An important feature of reaction scheme (2) is that the reaction species of GL is not a monoanionic species (AH), but a dianionic one (A), even though both are in equilibrium. Binding of AH to the polymer did not satisfy the pH-stat data at all. This is coincident with the fact that the monovalent ion hardly binds to the polymer. The estimated value of the stoichiometric parameters ($n=0.45$) implies that one dianion (A) binds with two residues of PLL. These values from the pH-stat data also satisfy the results of the equilibrium dialysis. Hereafter, we use $n=0.5$ as a meaningful value in the data analysis. Generally, equilibrium dialysis experiments also give the binding parameters. In the present studies, however, we used the data only for confirming the binding parameters obtained from the pH-stat experiments, due to the relatively great experimental error in the dialysis data. Meanwhile, the data concerning the pH change on the complexation also give the binding constant (K_{ov}) as can be seen in Fig. 5(b) (see Appendix 2). In this study we estimated the binding constant (K_{ov}) based on the pH change data for all systems except for the PLL–GL system.

Upon analyzing the kinetic data of the PLL–GL system, we examined many models. Among these, we propose the following reaction scheme as the best model for the complexation reaction, with accounts for the proton-uptake process:

$$L_1 + A \underset{(i)}{\overset{K_1}{\rightleftarrows}} C_1 \underset{(ii)}{\overset{K_2}{\rightleftarrows}} C_2 \underset{(iii)}{\overset{K_3}{\rightleftarrows}} L_2 + A \tag{I}$$

with

$$K_1=\frac{[C_1]}{[L_1][A]}, \quad K_2=\frac{[C_2]}{[C_1]}=\frac{k_{+2}}{k_{-2}}, \quad K_3=\frac{[C_2]}{[L_2][A]}, \tag{4}$$

$$[PLL_0]=2([L_1]+[L_2]+[C_1]+[C_2]), \tag{5}$$

$$[D_0]=[AH_2]+[AH]+[A]+[C_1]+[C_2], \tag{6}$$

and

$$K_{ov}=\frac{K_1K_3(1+K_2)}{K_1K_2+K_3}. \tag{7}$$

Table 1. Observation of the Kinetic Process and pH Change on the Polymer Complex Formation

System [a]	Observation of the pH change: Kinetic process (Proton uptake)	Observation of the pH change: ΔpH [b] (Total proton release)
A: Polymer–polymer system		
PLL (DP460)–PGA(DP250)	Observed	−1.01
–PGA(DP60)	Observed	−1.03
–PGA(DP10)	Observed	−0.89
B: Polymer–small molecule system		
PLL (DP460)–acetic acid	Not observed	ca. 0
–propionic acid	Not observed	ca. 0
–malonic acid	Observed	−0.25
–glutaric acid	Observed	−0.23
PGA (DP250)–methylamine	Not observed	ca. 0
–ethylamine	Not observed	ca. 0
–ethylenediamine	Observed	−0.15
–1,3-propanediamine	Observed	−0.14
–1,4-butanediamine	Observed	−0.14
C: Polymer-metal system [c]		
PGA (DP250)–Cu^{2+}	Observed	−0.92
–Ca^{2+}	Observed	−0.20
–Na^{+}	Not observed	ca. 0

a) Concentration of all the compounds was 1×10^{-4} M and initial pH was 5.5. b) The pH change was estimated by $\Delta pH=pH_{final}-pH_{initial}$; where pH_{final} and $pH_{initial}$ imply the pH value after and before complex formation, respectively. c) Though the kinetic process was observed, the mechanism was not examined in this paper.

In Eq. I, (i) implies the binding process between PLL and GL, where L_1 and C_1 denote the free and bound sites, respectively; (ii) represents the intramolecular process of the complex; (iii) represents the dissociation process. Equations 5 and 6 show the mass-conservation law for PLL and GL, respectively, where the binding of two residues of PLL with an ion of A species is adopted. In the case that the binding and dissociation processes of (i) and (iii), along with the protolysis reaction of A in Eq. I, are faster than the intramolecular process (ii), the rate equation for the intramolecular process is given by

$$\frac{d([L_2]+[C_2])}{dt} = k_{+2}[C_1] - k_{-2}[C_2] \tag{8}$$

and the relaxation time for the process can be written as

$$\tau^{-1} = k_{+2}\mathbf{A} + k_{-2}\mathbf{B} \tag{9}$$

with

$$\mathbf{A} = \frac{K_1([A]\mathbf{Y}+[L_1])}{\mathbf{Z}}, \tag{10}$$

$$\mathbf{B} = \frac{K_3\{(1+K_1[A])\mathbf{X}+[L_2](K_1-K_3)\}}{\mathbf{Z}(K_1-K_3)}, \tag{11}$$

$$\mathbf{X} = 1 + \frac{K_1[L_1]+K_2[L_2]}{1+K_1[A]} + \frac{K_{a2}[H]\{1+K_{a1}([H]+[AH])\}}{1+2K_{a1}[AH]+K_{a2}[A](1+2K_{a1}[H])},$$

$$\mathbf{Y} = \frac{[A](K_3-K_1)(K_1[L_1]+K_3[L_2])}{(1+K_1[A])\{(1+K_3[A])\mathbf{X}+[A](K_1-K_3)\}},$$

and

$$\mathbf{Z} = \frac{1+K_1[A]+K_3[A]\{(1+K_1[A])\mathbf{X}+[L_2](K_1-K_3)\}}{[A](K_1-K_3)}.$$

Prior to an analysis of the kinetic data using Eq. 9 we determined the value of K_1 based on the reaction strength data of the first binding process, of which only the reaction strength ($\gamma=-\Delta R/R$ in Fig. 6) was estimated, because of the resolution time of the present apparatus. Details concerning the determination of K_1 can be found in Appendix 3. Equation 9 is converted to

$$\frac{\tau^{-1}}{\mathbf{B}} = k_{+2}\frac{\mathbf{A}}{\mathbf{B}} + k_{-2}. \tag{12}$$

Assuming the value of K_2 (at this moment, all equilibrium constants are fixed by Eq. 7, the concentration of all the species at equilibrium can be calculated. Accordingly, plotting the left-hand side of Eq. 12 against the concentration term of the right-hand side gives the rate constants (k_{+2} and k_{-2}) from the slope and intercept of the fitted line, respectively. As a judge of the fitting, we used both the good linearity of the plot using Eq. 12 and the coincidence of the assumed value of K_2 with the calculated one from k_{+2} and k_{-2}. The best-fitting result is shown in Fig. 7(a). A similar analysis was also applied to the PLL–malonic acid (ML) system; its result is shown in Fig. 7(b). The evaluated parameters are listed in Table 2.

ii) PGA–DAM Systems: As can be seen in Fig. 4, the relaxation time was independent of the con-

Table 2. The Equilibrium and Kinetic Parameters for the Polymer Complex Formation

System	n[a)]	K_{ov} / M^{-1}	K_1 / M^{-1}	K_3 / M^{-1}	K_2	k_{+2} / s^{-1}	k_{-2} / s^{-1}	K_{2kin}[b)]
A: PLL–DCA system	0.5	($\times 10^5$)	($\times 10^5$)	($\times 10^5$)				
–glutaric acid		1.7±0.5	2.8±0.6	1.6±0.5	7.5±0.5	0.73±0.6	0.1±0.05	7.3
–malonic acid		1.2±0.5	2.5±1.2	1.1±0.7	7.5±0.8	1.37±0.2	0.18±0.1	7.6
B: PGA–DAM system	0.5	($\times 10^3$)	($\times 10^4$)	($\times 10^3$)				
–ethylenediamine –propanediamine		4.0±0.5	1.5±0.5	2±0.5	0.63±0.5	1.8±1.0	2.9±0.5	0.62
C: PGA–PLL system	1.0	($\times 10^5$)	($\times 10^5$)	($\times 10^5$)				
		1.7±0.5	6.5±0.6	1.5±0.5	6.8±2	3.1±2.0	0.5±1.0	6

a) n implies the number of binding sites per one residue of polymer. b) K_{2kin} was estimated from k_{+2}/k_{-2}.

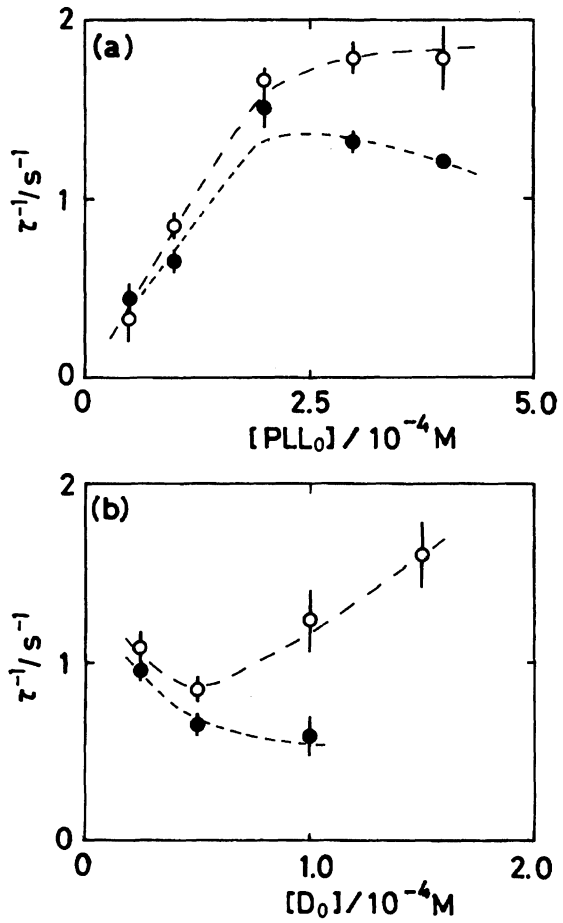

Fig. 3. The concentration dependence of the time constant for the PLL–DCA system. (a) $[PLL_0]$ dependence at the concentration of dicarboxylic acid $[D_0]=5.0\times10^{-5}$ M. (b) $[D_0]$ dependence at $[PLL_0]=1.0\times10^{-4}$ M. (○) for malonic acid, and (●) for glutaric acid. DP of PLL is 460.

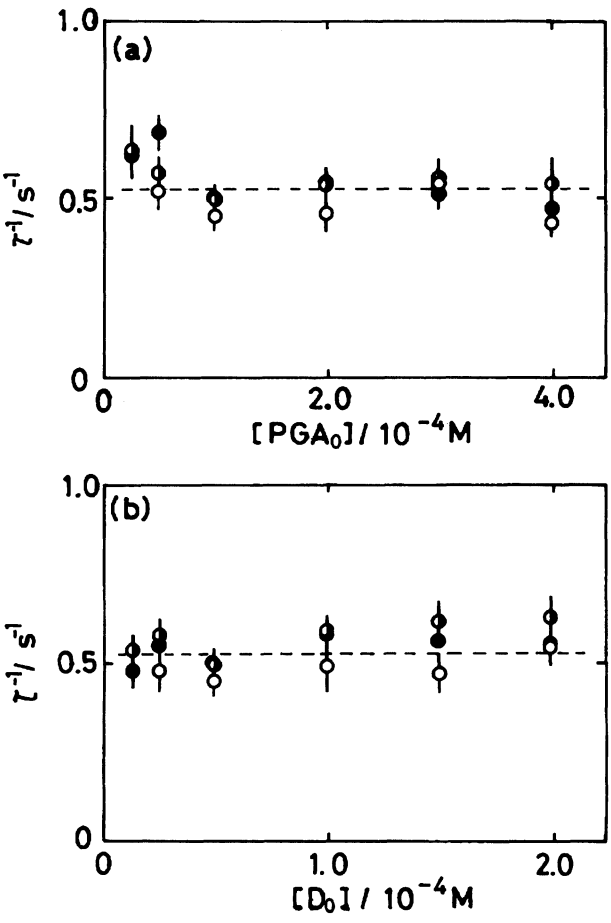

Fig. 4. The concentration dependence of the time constant for the PGA–DAM system. (a) $[PGA_0]$ dependence at $[D_0]=5.0\times10^{-5}$ M. (b) $[D_0]$ dependence at $[PGA_0]=1.0\times10^{-4}$ M. (○) ethylenediamine, (◑) propanediamine, and (●) butanediamine. DP of PGA is 250.

centration of both PGA and DAM, as well as the kind of the diamines, such as ethylenediamine, 1,3-propanediamine, and 1,4-butanediamine. The amount of proton release during complex formation was also the same for all of the diamines examined, as can be seen in Table 1.

These resutls may imply that under the present experimental conditions the reaction of all the diamines with PGA proceeds by the same mechanism. In contrast to PLL–DCA system, a polymer of PGA is in protolysis equilibrium, and the diamine molecules are almost protonated as a dicationic form at pH 5.5. Then, the

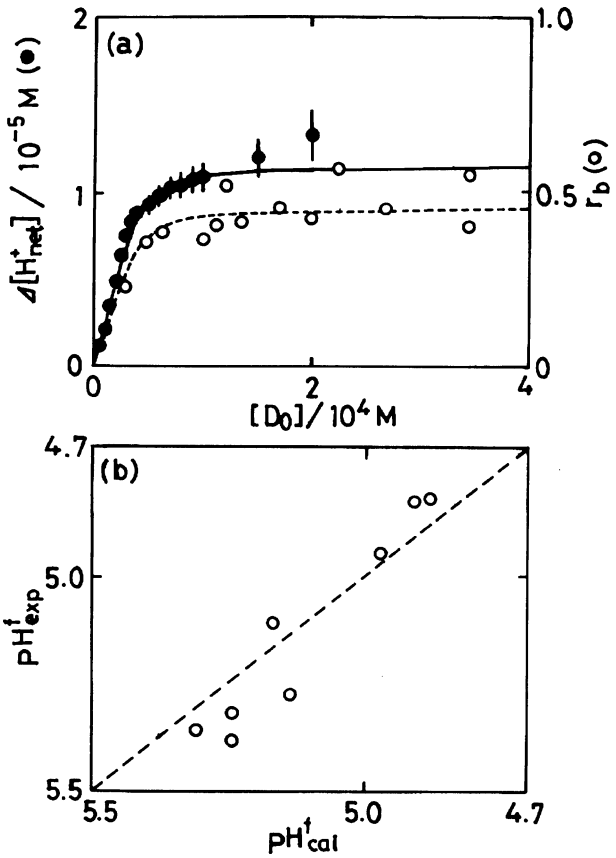

Fig. 5. The results of pH-stat titration (●) and equilibrium dialysis (○) and the estimation of binding parameters for PLL–glutaric acid system. (a) Solid and dashed lines show the theoretical characteristics using the estimated parameters. (b) The overall binding constant $K_{ov}=(1.7\pm0.5)\times10^5$ M^{-1} for the PLL–glutaric acid system was estimated from the pH change data. Details as to the estimation of K_{ov} can be seen in Appendix.

overall binding constant (K_{ov}) was estimated from the proton-release data according to the following reaction scheme:

$$GH \overset{K_G}{\rightleftarrows} G + H^+, \tag{13}$$

and

$$P + B \overset{K_{ov}}{\rightleftarrows} C, \tag{14}$$

where Eq. 13 represents the protolysis reaction of PGA in the residue unit, and Eq. 14 the complexation between the binding site on the PGA and the dicationic species of diamine. The equilibrium constants for each reaction and mass-conservation law are represented as follows:

$$K_G = \frac{[GH]}{[G][H]}, \quad K_{ov} = \frac{[C]}{[B][P]}, \tag{15}$$

$$[PGA_0] = [GH] + 2\{[P] + [C]\}, \tag{16}$$

$$[G] = 2[P], \tag{17}$$

$$[D_0] = [B] + [C], \tag{18}$$

and

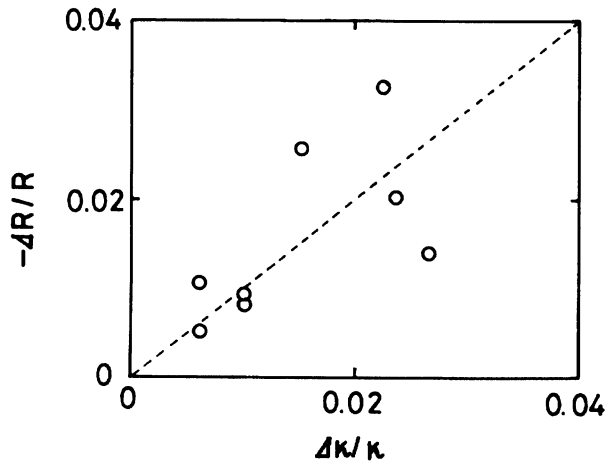

Fig. 6. Estimation of the binding constant K_1 from the reaction strength ($-\Delta R/R$) for the PLL–glutaric acid system. ($\Delta K/K$) denotes the calculated reaction strength.

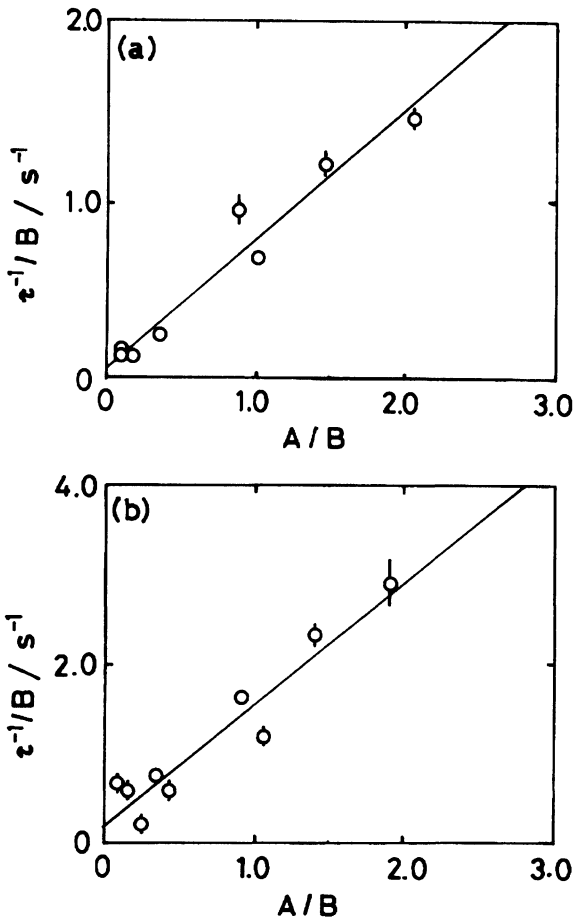

Fig. 7. A plot of the relaxation time to estimate the rate constants with reference to Eq. 12 for the reaction Eq. I. (a) for the PLL–glutaric acid system. (b) for the PLL–malonic acid system.

$$[H_0] = [GH] + [H], \tag{19}$$

where the protolysis equilibrium constant was deter-

mined to be $K_G=1.6\times10^6$ M^{-1} from pH titration experiments of PGA, and $n=0.5$ was used as a stoichiometric coefficient of the PGA in complex formation. From the kinetic data analysis, we can propose the following scheme instead of Eq. I for the complexation between PGA and DAM:

$$G_1 + B \underset{(i)}{\overset{K_1}{\longleftrightarrow}} C_1 \underset{(ii)}{\overset{K_2}{\longleftrightarrow}} C_2 \underset{(iii)}{\overset{K_3}{\longleftrightarrow}} G_2 + B \qquad \text{(II)}$$

with

$$[PGA_0] = [GH] + 2\{[G_1] + [G_2] + [C_1] + [C_2]\}, \qquad (20)$$

$$[D_0] = [B] + [C_1] + [C_2], \qquad (21)$$

and

$$[G] = 2\{[G_1] + [G_2]\}, \qquad (22)$$

where $[PGA_0]$ and $[D_0]$ denote the total concentration of PGA in the residue unit and diamine, respectively. In analogy with the PLL–DCA system, processes (i) and (iii) represent the binding and dissociation processes of dication of diamine (B) before and after the intramolecular processes of complex (ii). The relaxation time for the slow intramolecular process can be written as

$$\tau^{-1} = k_{+2}\mathbf{A} + k_{-2}\mathbf{B} \qquad (23)$$

with

$$\mathbf{A} = \frac{K_3[B]\mathbf{X}}{1 + K_3\{[B][G_2](1-\mathbf{X})\}}, \qquad (24)$$

$$\mathbf{B} = \frac{K_3[B]}{1 + K_3\{[B] + [G_2](1-\mathbf{X})\}}, \qquad (25)$$

and

$$\mathbf{X} = \frac{K_1\{1+K_G([G]+[H])\}\{1+K_3([G_1]+[G_2])\}+K_3[B](1+K_G[G])}{K_3\{1+K_G([G]+[H])\}\{1+K_1([G_1]+[G_2])\}+K_1[B](1+K_G[G])}. \qquad (26)$$

After estimating the bind constant (K_1) based on the reaction strength by the method noted above, the concentration dependence of the relaxation time was examined. The best-fitting result is shown in Fig. 8, and the estimated values, which are the same for all of the diamines, are listed in Table 2.

iii) PGA–PLL System: Concerning the reaction mechanisms that were clarified for the polymer–divalent ion complex formation of the PLL–DCA and PGA–DAM systems, the reaction mechanism for the polymer–polymer complex formation of the PGA–PLL system could be barely examined. In this system, the protolysis reaction of PGA and the overall reaction between PGA and PLL can be written as

$$GH \overset{K_0}{\longleftrightarrow} G + H^+ \qquad (27)$$

and

$$G + L \overset{K_{ov}}{\longleftrightarrow} C, \qquad (28)$$

where K_G was the same as that in Eq. 15, and K_{ov} could be estimated based on the proton-release data

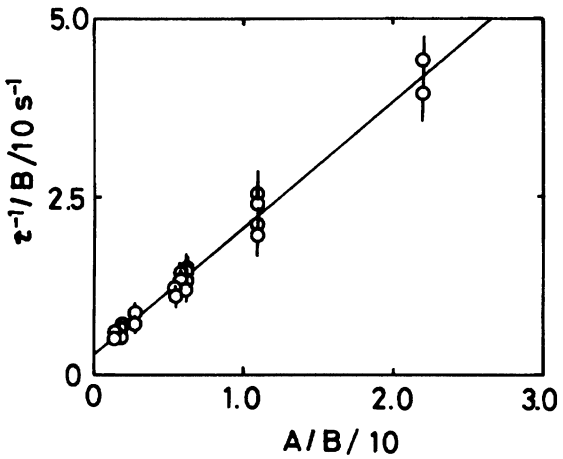

Fig. 8. A plot of the relaxation time to estimate the rate constants with reference to the Eq. II for the PGA–diamine system.

concerning complex formation. The mechanism proposed above for the PLL–DCA and PGA–DAM systems suggests that the proton uptake observed in the PGA–PLL system arises from dissociation of PGA after the intramolecular process of the complex. However, we still have three possible Schemes in which both of the polymers or one of them change their final state after complex dissociation:

$$L_1 + G_1 \longleftrightarrow C_1 \longleftrightarrow C_2 \longleftrightarrow L_2 + G_2 \qquad \text{(IIIa)}$$

with the mass conservation law;

$$[PLL_0] = [L_1] + [C_1] + [C_2] + [L_2],$$

and

$$[PGA_0] = [GH] + [G_1] + [C_1] + [C_2] + [G_2].$$

$$L_1 + G \longleftrightarrow C_1 \longleftrightarrow C_2 \longleftrightarrow L_2 + G \qquad \text{(IIIb)}$$

with

$$[PLL_0] = [L_1] + [C_1] + [C_2] + [L_2],$$

and

$$[PGA_0] = [GH] + [G] + [C_1] + [C_2].$$

$$G_1 + L \underset{(i)}{\overset{K_1}{\longleftrightarrow}} C_1 \underset{(ii)}{\overset{K_2}{\longleftrightarrow}} C_2 \underset{(iii)}{\overset{K_3}{\longleftrightarrow}} G_2 + L \qquad \text{(IIIc)}$$

with

$$[PLL_0] = [L] + [C_1] + [C_2],$$

and

$$[PGA_0] = [GH] + [G_1] + [C_1] + [C_2] + [G_2].$$

Eq. IIIa implies that both PGA and PLL change their states after complex dissociation. However, we could not analyze our kinetic data with this Scheme because of a lack of quantitative information concerning the species of G_2 and L_2. Eq. IIIb, which includes the change of

PLL alone after dissociation, did not satisfy the kinetic data, and Eq. IIIc, which includes an alternation of PGA after complex dissociation, was the most satisfactory one. The relaxation time for the slow intramolecular process of (ii) in Eq. IIIc is also represented by Eqs. 23 to 26 with minor changes of the following concentration terms:

$$[G] = [G_1] + [G_2], \tag{29}$$

and

$$[B] = [L], \tag{30}$$

where a stoichiometric coefficient for complexation of n=1.0 (which means one residue of PGA and PLL binds with each other) was used. The best-fitting result of the kinetic data is represented in Fig. 9, and the estimated parameters are listed in Table 2.

Discussion

By analyzing the kinetic data for the three systems of PLL–DCA, PGA–DAM, and PGA–PLL it was clarified that proton-release from acidic molecule occurs during the first binding process, and that the dissociation of the complex induced by some kind of intramolecular process of the complex gives rise to proton-uptake. For a more detailed discussion of the intramolecualr process, we measrued the CD spectra for each system both before and after complex formation. At pH 5.5, PGA has a helix content of about 76%, while PLL has no helical form by itself. From the CD measurements for the complex, the following were confirmed (Data not shown): (i) no helix formation occurred in the PLL–DCA system, (ii) the helix content decreased in the PGA–DAM system, and (iii) although the helix content increased in the PGA–PLL system, its increments could not be divided into respective contributions of PGA and PLL. If the change in the CD spectra is assumed to result from the PGA alone, we could estimate the increment

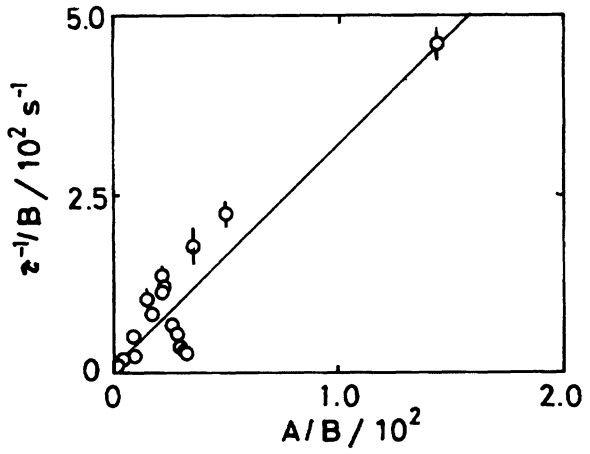

Fig. 9. A plot of the relaxation time to estimate the rate constants with reference to the Eq. IIIc for the PGA–PLL system.

of the helix contents from 76 to 85%. We then applied the CD dectection stopped-flow method to the PGA–PLL system, but could not observe any change in the CD signal in the range 50 ms to 3 min. This result implies that, even if a conformational change such as helix formation occurs, it must be faster than 50 ms, and that the observed proton-uptake process is not accompanied by any change in the helix contents of the polymer. Accordingly, the intramolecular process is not specific for the secondary conformational change, but may be some kind of tertiary structural change.

Among the estimated overall binding constants (K_{ov}, as shown in Table 2) the values for the PLL–DCA system are comparable with that for the PLL–PGA system, and larger than that for the PGA–DAM system by at least one order of magnitude. The comparable binding constants for the PLL–DCA and PLL–PGA systems suggest that the stability of these complexes is governed mainly by the PLL; however, even the DP=250 of PGA does not show any significant effect on the stability of their complex with the PLL. As for the origin of such high stability of complexes by the PLL, we can point out the following three possible reasons: (1) the high electrostatic positive charge density of PLL at the acidic pH regions, (2) the longer chain length (DP=460) of PLL than that of PGA (DP=250), and (3) the longer side chain length of PLL than PGA. Meanwhile, the relatively low stability of the PGA–DAM complex seems to arise from incomplete dissociation of PGA at the present pH region and the small DP (250); the helical conformation of PGA is also a factor. Accordingly, for PLL–PGA complex formation, the DP of PGA more than those of PLL is expected to have an effect on their stability. As for the K_2 obtained in Table 2, the value only for the PGA–DAM system is less than unity, which means that complex C_1 is more stable than C_2 in reaction Eq. II. Although we cannot explain this result explicitly at present, it may be related to a decrease in the helix contents of PGA at the first complexation process.

The mechanism of the proton behavior through polymer complexation can be explained in the following manner. As for the proton release, after electrostatic binding of COO^- with NH_3^+ induces a shift of the protolysis equilibrium of carboxylic acid, a proton release from undissociate COOH occurs. However, regarding the proton-uptake process, the complex formed by fast electrostatic binding between counter-chaged ionic species is not sufficiently stable, and therefore must convert its structure into the final stable state. The smaller binding constant K_3 (than K_1) for all of the systems accounts for the dissociation in some part of complex C_2 leading to proton-uptake after complex dissociation. Concerning conversion as an intramolecular process, the dissociation of the complex in part is followed, and then proton uptake continues. In other words, complex C_1 produced by the electrostatic and probably the cooper-

ative interactions between two counter-charged species in Eqs. I, II, and IIIc may be stable in the sense of enthalpy, but unstable in entropy. The rearrangement of the polymer then continues while seeking a more stable conformation. The rate constants, k_{+2} and k_{-2}, for the rearrangement of the polymer complex are in 0.1 to 3.1 s^{-1} for the three systems (Table 2). At present, the values of the rate constants do not show any systematic feature, but may suggest that, as a general property of an ionic polymer, especially of a linear polymer, the rearrangement of the polymer complex after electrostatic binding continues over a time range of seconds.

As to why a counter-charged ion of divalent or more is specific for the proton behavior observed in the present work, we can reasonably deduce from the pH-change data shown in Table 1 that a monovalent ion cannot interact sufficiently strongly with an ionic polymer. The interaction of counter-charged ions of divalent or more with an ionic polymer arises from the strong electrostatic force and from a linkage or the chelation structure of multivalent ions on the polymer, as suggested by Tsuchida et al.[21—25] For such a linkage on the polymer, divalency is at least requested as reported for the system of a divalent metal ion–poly (acrylic acid) which makes a linkage of the form COO–Metal–OOC.[3] The unstable intermediate complex in the fast step then converts itself into a stable one through the intramolecular process accompanying a break down of the binding in part. This rearrangement process must be a rate-determining step of the complex formation and proton-uptake process. For the system of weak and strong polyelectrolytes,[26] it was reported that the complexation proceed through two processes: a fast binding process and a slow intramolecular process.[9,25] In particular, Okubo et al., using the conductance stopped-flow technique, observed two reaction curves of a rapid increase and a slow decrease in conductance. They did not, however, mention the relationship between the conductance change and proton behavior. From the present investigations, it can be explained that the conductance changes in their experiments corresponded to the proton processes.

In conclusion, proton release and uptake occur by a shift of the protolysis equilibrium of carboxylic acid due to both the binding of counter-charged ions and a partial dissociation of complex after a rearrangement of the complex. The present results suggest that a similar proton behavior may take place in many biochemical systems, such as the protein–protein interaction, enzyme–substrate interactions,[15,16] and proton pumps[17,18] in which the behavior of the proton is very important.

Appendices

Appendix 1. According to the reaction given by Eq. 1 in the text, the protolysis equilibrium constants (K_{a1} and K_{a2}) are given by

$$K_{a1} = \frac{[AH_2]}{[AH][H]}, \quad K_{a2} = \frac{[AH]}{[A][H]}. \tag{A1}$$

From the mass-conservation law,

$$[P_0] = ([P] + [C])/n, \tag{A2}$$

and

$$[D_0] = [AH_2] + [AH] + [A]. \tag{A3}$$

The amount of the added NaOH (ΔH_{added}) to bring the pH of the complex solution back to 5.5 is given by

$$\Delta H_{added} = \frac{K_{a1}[H][C]\{2[H]K_{a1} + 1\}}{K_{a1}K_{a2}[H]^2 + K_{a2}[H] + 1}. \tag{A4}$$

Using these equations along with Eq. 3 in the text, K_{ov} and n were determined so as to satisfy the experimental results of ΔH_{added} against $[D_0]$.

Applendix 2. As for the reaction given by Eq. 2 in the text, the overall binding constant and mass-conservation law can be written as

$$K_{ov} = \frac{[C]}{[P][A]}, \tag{A5}$$

$$[PLL_0] = 2\{[P] + [C]\}, \tag{A6}$$

$$[D_0] = [AH_2] + [AH] + [A] + [C], \tag{A7}$$

$$[H_0] = 2[D_0] - [NaOH]_{added} = 2[AH_2] + [AH] + [H]. \tag{A8}$$

Here, $[NaOH]_{added}$ denotes the added concentration of NaOH to adjust the pH of the solution to 5.5 before complex formation (practically before mixing). From these equations, along with Eq. A1, the value of K_{ov} was determined so as to obtain a linear relationship between the two final pHs, i.e., the experimentally determine pH^f_{exp} and the calculated pH^f_{cal}.

Appendix 3. The reaction strength (γ) of the first binding process can be represented by the following equation in general form using the molar conductivity and concentration change:

$$\gamma = -\frac{\Delta R}{R} = \frac{\Delta K}{K} = \frac{F\sum|z_i|\mu_i\Delta C_i}{F\sum|z_i|\mu_i C_i}, \tag{A9}$$

where R and K denote the electric resistance and conductivity of the solution, respectively. F is the Faraday constant, z_i the charge of the ionic species, μ_i the activity coefficient, and C_i the concentration of ionic species i. ΔC_i is the concentration change in the ionic species during the first binding reaction. We adopted the hydrogen ion as a variable ionic species, since the conductivity change closely corresponds to the change in the hydrogen ion. Assuming the value of the first binding constant (K_1), the concentration of each reaction species just after the first binding can be estiamted; one can then calculate the reaction strength of the first process with reference to Eq. A9. The value of K_1 was determined so as to give a good linear correlation between the experimentally obtained reaction strength ($-\Delta R/R$) and the calculated one ($\Delta K/K$).

References

1) A. Veis, "Biological Polyelectrolytes," Marcel Dekker, New York (1970), pp. 211—271.

2) R. A. Gelman, W. B. Rippon, and J. Backwell, *Biopolymers*, **12**, 541 (1973).

3) F. Oosawa, "State of Binding of Counter Ions," in "Polyelectrolytes," Marcel Dekker, New York (1971), p. 33.

4) C. S. Cho, T. Komoto, and T. Kawai, *Makromol. Chem.*, **180**, 1951 (1979).
5) H. Nakatani, Y. Uehara, and K. Hiromi, *J. Biochem.*, **78**, 611 (1975).
6) W. L. Mattice, R. W. McCord, and P. M. Shippey, *Biopolymers*, **18**, 723 (1979).
7) E. Tsuchida, Y. Osada, and K. Abe, *Makromol. Chem.*, **175**, 593 (1974).
8) H. Ohno, H. Matsuda, and E. Tsuchida, *Makromol. Chem.*, **182**, 2267 (1981).
9) T. Okubo, K. Hongyo, and A. Enokida, *J. Chem. Soc., Faraday Trans. 1*, **80**, 2087 (1984).
10) V. A. Izumrudov, T. K. Bronich, A. B. Zezin, and V. A. Kabanov, *J. Polym. Sci., Polym. Lett. Ed.*, **23**, 439 (1985).
11) M. Rinaudo and A. Domard, *J. Am. Chem. Soc.*, **98**, 6360 (1976).
12) A. Domard, M. Rinaudo, and C. Rochas, *J. Polym. Sci., Polym. Phys. Ed.*, **19**, 673 (1979).
13) C. Rochas, A. Domard, and M. Rinaudo, *Eur. Polym. J.*, **16**, 135 (1980).
14) T. Nakatsuka and T. Sano, *Chem. Lett.*, **1988**, 737.
15) A. Domard and M. Rinaudo, *Macromolecules*, **13**, 898 (1980).
16) A. Domard and M. Rinaudo, *Macromolecules*, **14**, 620 (1981).
17) S. E. Halford, *Biochem. J.*, **149**, 411 (1975).
18) Y. Kagawa, *J. Biochem.*, **95**, 295 (1984).
19) T. Ikeda, J. Nakahara, M. Sasaki, and T. Yasunaga, *J. Colloid Ineterface Sci.*, **97**, 278 (1984).
20) T. Nakatsuka, M. Nakamura, and T. Sano, *Bull. Chem. Soc. Jpn.*, **61**, 799 (1988).
21) E. Tsuchida, K. Abe, and M. Honma, *Macromolecules*, **9**, 112 (1976).
22) E. Tsuchida, Y. Osada, and K. Abe, *Makromol. Chem.*, **175**, 583 (1974); **175**, 593 (1974).
23) E. Tsuchida, *Makromol. Chem.*, **175**, 603 (1974).
24) E. Tsuchida, Y. Osada, and K. Abe, *J. Polym. Sci., Polym. Chem. Ed.*, **14**, 767 (1976).
25) K. Abe, M. Koide, and E. Tsuchida, *Polym. J.*, **9**, 73 (1977).
26) The substances were sodium polyacrylate and polybrene, polyethylenimine and sodium poly(ethylenesulphonate) in the Ref. 9, and poly(methacrylic acid) and poly(*N*,*N*,*N*′,*N*′-tetramethyl-*N*-*p*-xylylenealkylenediammoniumdichloride) in the Ref. 21.